Numerical Investigation of a Globe Control Valve and Estimating its Loss Coefficient at Different Opening States

Saber Rezaey

Faculty of Mechanical Engineering, Tarbiat Modares University, Tehran, Iran
E-mail: saberrezaey@modares.ac.ir

Received 12 December 2020; Accepted 04 May 2021;
Publication 19 May 2021

Abstract

One of the most important components of fluid transmission systems is a control valve located in the pipelines of oil, gas, etc. The primary purpose of this valve is to control the rate of fluid flow passing through it under pressure changes and the most important issue is to investigate the flow's characteristics in order to achieve a proper geometry to control the flow rate and pressure as desired. The valves used in pipelines add to the overall head loss of the system. Therefore, valves with proper geometry can reduce these minor losses and finally decrease total energy losses. In this paper, a globe control valve is modeled and then numerically investigated to extract its functional relation, which relates pressure ratio to inlet Reynolds number, and estimate its loss coefficient at the valve's different opening states which have not been addressed completely before and can be beneficial for the selection and usage of globe valves under certain conditions. According to the results, it is found that pressure ratio and loss coefficient are functions of inlet velocity and the valve's opening state's percentage, which are directly related to the valve's geometry. When the valve opens, the rate of change in pressure ratio and loss coefficient are very sharp. Gradually, this rate decreases and the results tend to the final value at the valve's fully opened state.

European Journal of Computational Mechanics, Vol. 29_4–6, 549–576.
doi: 10.13052/ejcm1779-7179.294610

Keywords: Fluid, globe valve, computational fluid dynamics (CFD), pressure, loss coefficient.

1 Introduction

Control valves are types of industrial valves that are widely used in various industrial fields such as oil and gas industries, power plants, petrochemicals, and water transmission systems. These types of valves can be opened or closed by the command of the controller. These valves are used to control pressure, temperature, flow rate, or height of liquids. The force required to open and close the valve in the control valves can be electrically, hydraulically, or pneumatically.

These valves come in many different types, including globe, ball, butterfly, and plug valves. Globe valve, also called a spherical valve, is used to adjust the flow rate and pressure of the fluid passing through it. In these valves, fluids outlet pressure is relevant to the number of rounds of the valve's handles. Globe valve is such a linear valve that is shaped like a disk. The end of this valve is made like a sphere or cone, and by placing on a seating ring can make the path fully opened, fully closed, or opened to a certain extent. For this reason, the globe valve is used in transmission lines along with other valves.

Globe Valves are usually made of metallic alloys or metal. A plug is the main part of a globe valve which is generally made of steel, grey iron, or ductile iron. Also, packing is usually produced from graphite, rubber, or PTFE. Figure 1 gives an overview of a globe valve.

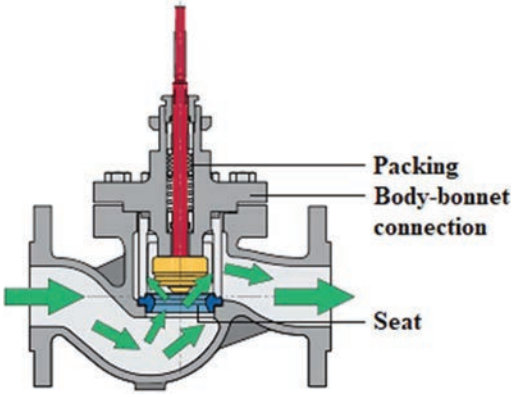

Figure 1 Schematic of a globe valve.

The geometry of a valve has a direct effect on the fluid flowing through it. If the geometry of the designed valve is inadequate, this will increase the losses and thus reduce the efficiency of the fluid transmission path. Therefore, designing an optimal geometry that avoids energy loss and severe pressure drop can be an attractive concern for mechanical engineers. Specifically, about a globe valve, this clever design requires sufficient knowledge of how fluid passes through it. In the present paper, a globe valve is modeled and then numerically investigated to derive its functional relation and estimate its loss coefficient to detect how fluid passes through it.

Despite control valves have a significant effect in a control loop, little study has been done on them. For calculating flow and pressure relations, The Crane Company's technical paper [1] attempted to analyze losses through valves and expressed analytical data for fully opened valves. Davis, J.A., and Stewart, M. [2, 3] used both numerical and experimental methods for analyzing a globe control valve and showed that simplified CFD analysis is useful. The study showed that the flow coefficient at the valve's different opening states could be predicted. Lin et al. [4] studied the cone angle of a globe control valve and found that the valve's opening state affects the cone angle. Long and Guan [5] studied an angle-seat valve experimentally and expressed a method for obtaining the valve flow coefficient and resistance coefficient. They assumed air as the working fluid and expressed the valve flow coefficient and resistance coefficient. Chern and Wang [6] studied a ball valve and investigated the effect of V-port on the performance of the valve with both numerical and experimental methods. They indicated that however, V-ports increase the pressure loss, they relate the flow rate to the valve's opening state and make the ball valve to be linearly controllable. Del Toro et al. [7] analyzed a butterfly valve and investigated its loss coefficient and flow coefficient at different opening states under different flow conditions with a numerical method. Their results showed that CFD can greatly simulate the valve performance factor at 30 to 60 degrees opening states. Md. Farhadul Haque et al. [8] Studied plastic ball valves and determined minor head loss of the valve for different fluid inlet velocities experimentally. They showed that as the Re number increases, the minor loss coefficient decrease. Tabrizi et al. [9] developed a finite volume-based code and simulated a ball valve's performance at different opening states. They found that the valve's opening state has a great effect on the valve's performance. S. F. Moujaes et al. [10] developed a three-dimensional computational fluid dynamics model to simulate fluid flow in a flanged ball valve at different opening states. They used the simulation to calculate the loss coefficient and

the flow coefficient of the modeled valve. Results showed that the simulations agreed with recent experimental results and indicated that the flow coefficient increases as the valve's opening state changes from a fully closed to a fully opened state. Cui et al. [11] studied the flow characteristics in a ball valve. The main purpose of this work was to investigate the flow characteristics of the modeled valve during the opening and closing process. They found that if the opening or closing time increases, the results tend to steady state condition. V. G. Fester et al. [12] investigated the loss coefficient for five types of diaphragm valves for Newtonian and non-Newtonian fluids and also various inlet Re numbers. They showed that the valve's diameter had a great influence on the loss coefficient. Takeyoshi et al. [13] investigated the performance of a butterfly valve and developed a theoretical loss coefficient formula and predicted cavitation stages using the formulated loss coefficient. Qian J.-Y. et al. [14] simulated a pilot-control globe valve by CFD method. They analyzed three different opening processes and found the best design for the valve and also investigated the relationship between inlet pressure and the valve's opening state. Jin Z.-J. et al. [15] used CFD method to analyze pressure drop and minor loss of a pilot-control globe valve at different inlet velocities. They found that the valve diameters affect the loss coefficient and the pressure drop. Also, they suggested an expression for the pressure drop of the modeled valve. Lee, J. H. et al. [16] investigated the flow coefficient for a pan check valve by using computational fluid dynamic analysis and calculated head loss at different inlet velocities at the optimum design. They realized that the length of the supporting beam had a great influence on the fluid performance and also predicted the optimum length for the supporting beam. Song, X. et al. [17] modeled and investigated a butterfly valve by using numerical simulation. Their results showed that this valve works well in 3 m/s inlet velocity. Xinbei, Lv. et al. [18] studied servo valves and predicted the vibration characteristics of them. Their results indicated that in servo valves, the spring tube has a great influence on the dynamic response of the system. Also, further studies [19, 20] were done on the vibrational frequencies of different systems to model the dynamical behavior and stability regions of the systems under various environmental changes. Kerboua, Y. et al. [21] developed a computational model and investigated the dynamic behavior of coupled fluid-structure systems. Also, they checked out the effect of physical parameters on the dynamic behavior of the modeled system. They showed that the developed approach can be used for various plate and shell structures. Ghazanfari, V. et al. [22] used an Implicit Coupled Density-Based solver in

OpenFOAM to simulate flow over a 2-D cylinder and found that the solver has a good accuracy.

Two crucial factors in valves are fluids velocity and the valve's loss coefficient. Having enough information about these factors can lead us to design the best geometry for valves and finally reduce energy losses. In this paper, the main objective is to find a relationship between inlet velocity ($\mathrm{Re_{in}}$) and pressure ratio ($\mathrm{P_{out}/P_{in}}$). This relation can be a functional relation for the modeled globe valve. Moreover, estimating the loss coefficient at different opening states can be useful in piping systems. First of all, a three-dimensional model is designed and analyzed. Finally, it is seen that the results generally agree with those mentioned above.

2 Theory

2.1 General Characteristics of Internal Flow

For internal flow, the most important dimensionless parameter is the Reynolds number

$$Re = \frac{\rho u D}{\mu} \tag{1}$$

This dimensionless number indicates whether a flow will be laminar or turbulent. The Flow will generally be laminar for $\mathrm{Re} \leq 2300$ and turbulent for larger values. The flow in a pipe with a constant diameter will be laminar or turbulent, depending on the value of the average velocity u. For laminar flow, dimensional flow analysis is used to determine the frictional loss in incompressible, steady, and extended fluid flow. Assume that the pressure drop is a function of the average velocity of the fluid flow, u, the pipe length, L, the diameter of the pipe, D, and the fluid viscosity, μ. The fluid specific weight and the density have not been assumed as parameters because for laminar flows they have not important effects on the pressure drop. Therefore, there isn't any presence of mass times acceleration and a component of weight in the following equations. Thus, $\Delta p = f(u, D, L, \mu)$. According to the dimensional analysis results, this flow can be expressed by the following dimensionless group:

$$\frac{D\Delta p}{\mu u} = \phi\left(\frac{L}{D}\right) \tag{2}$$

The Equation 2 can be true only if:

$$\phi\left(\frac{L}{D}\right) = C\frac{L}{D} \tag{3}$$

where *C* is a constant. By theoretical or experimental analysis, one can determine the value of *C*. For example, for a round pipe, $C = 32$. It can be useful to express a process by dimensionless quantities. For this purpose, and by substituting Equation (3) into Equation 2, the pressure drop for such flow can be written as $\Delta p = \frac{32\mu L u}{D^2}$. By dividing both sides by the dynamic pressure, the dimensionless form of pressure drop will be obtained as follows:

$$\Delta p = f\frac{L}{D}\frac{\rho u^2}{2} \tag{4}$$

where f is termed the friction factor. Therefore, for laminar fully developed pipe flow, the friction factor is expressed as:

$$f = \frac{64}{\mathrm{Re}} \tag{5}$$

The same method can be used for turbulent flow. For a horizontal and round pipe of diameter *D* and for incompressible and steady turbulent flow, the pressure drop can be written as $\Delta p = f(u, D, L, \varepsilon, \mu, \rho)$ where u is the fluid flow's average velocity, L is the length of pipe, and ε is a measure of the roughness. It is obvious that Δp depends on u, D, and L. Also, because of the effect of shear stress on the pressure drop, the dependence of Δp on the fluid properties μ and ρ should be taken into count. Hence, this flow can be expressed in terms of the following dimensionless group:

$$\frac{\Delta p}{\frac{1}{2}\rho u^2} = \frac{L}{D}\phi\left(\frac{\rho u D}{\mu}, \frac{\varepsilon}{D}\right) \tag{6}$$

As it is seen there are two differences between the results of pressure drop in laminar and turbulent flows. First, the Reynolds number, Re, and the relative roughness, $\frac{\varepsilon}{D}$, are present in the turbulent flow which wasn't taken into count in laminar flow. And second, in turbulent flow, the dynamic pressure, $\frac{\rho u^2}{2}$, is used to make the pressure dimensionless, but in laminar flow, viscous shear stress, $\frac{\mu u}{D}$, was used. Finally, Equation 4 will be obtained by using the friction coefficient definition. However, in turbulent flow, the coefficient of friction is defined as:

$$f = \phi\left(\frac{\rho u D}{\mu}, \frac{\varepsilon}{D}\right) \tag{7}$$

For turbulent flow, the dependence of the friction factor on the relative roughness and the Reynolds number is complicated and can't be computed easily. The results which are used in fluid mechanics are almost experimental

Table 1 Equivalent roughness for new pipes [23]

	Equivalent Roughness, ε	
Pipe	Feet	Millimetres
Riveted steel	0.003–0.03	0.9–9
Concrete	0.001–0.01	0.3–3.0
Wood stave	0.0006–0.003	0.18–0.9
Cast iron	0.00085	0.26
Galvanized iron	0.0005	0.15
Commercial steel (wrought iron)	0.0005	0.045
Drawn tubing	0.000005	0.0015
Plastic, glass	0.0 (smooth)	0.0 (smooth)

which was were carried out by J. Nikuradse in 1933. L. F. Moody along with C. F. Colebrook, associated the Nikuradse data with the relative roughness of pipe materials in a chart which is called Moody chart [23]. L. F. Moody and C. F. Colebrook results for different pipes roughness values are seen in Table 1.

The Moody chart indicates the dependence of f on the relative roughness and the Reynolds number. The nonlaminar part of the Moody chart can be expressed by the following equation [23]:

$$\frac{1}{\sqrt{f}} = -2\log\left(\frac{\varepsilon/D}{3.7} + \frac{2.51}{\mathrm{Re}\sqrt{f}}\right) \tag{8}$$

2.2 Minor Loss

Most pipe systems in addition to straight pipes have some additional components such as valves and bends which increase the overall head loss of the system. These additional losses are called minor losses. The head loss that occurs when the fluid passes through a valve is one of these important minor losses. A valve can control the flow rate by changing its geometry. When a valve's plug moves from the fully closed position to the fully opened position, the flow rate increases, and this change in the valve's geometry can affect the flow pattern. Therefore, according to the vast use of valves in pipe systems, the head loss through a valve is an important part of the pipe systems losses. In fact, when a valve is fully closed, the resistance against the flow is infinite. It can be very beneficial to describe these minor losses with a coefficient. This coefficient is called the loss coefficient, K_L, and is expressed as follows:

$$K_L = \frac{h_L}{u^2/2g} = \frac{\Delta p}{\frac{1}{2}\rho u^2} \tag{9}$$

Minor losses may be expressed in terms of the equivalent length, L_{eq}, of pipe that would have the same head loss for the same discharge flow rate. This relationship can be found by setting the Equations 4 and 9 equal to each other. This terminology yields the following equation.

$$L_{eq} = \frac{K_L D}{f} \tag{10}$$

The equivalent length of piping that will cause the same head loss as a particular component can be determined by multiplying the value of $\frac{L_{eq}}{D}$ for that component by the diameter of the pipe. The higher the value of $\frac{L_{eq}}{D}$, the longer the equivalent length of pipe.

3 Numerical Method

3.1 Physical Model

The purpose of this paper is to investigate the flow of water through a wrought-iron plate valve. For this purpose, SolidWorks is used to generate a globe valve model. The geometry of the valve designed by SolidWorks is Shown in Figure 2. The fluid flow passes through the inner part of the valve. Therefore, in order to simplify the flow analysis, parts of the valve that are not in contact with the fluid are removed, and the final simplified geometry is given in Figure 3.

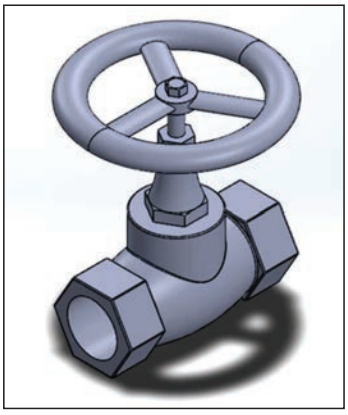

Figure 2 SolidWorks model of the globe valve.

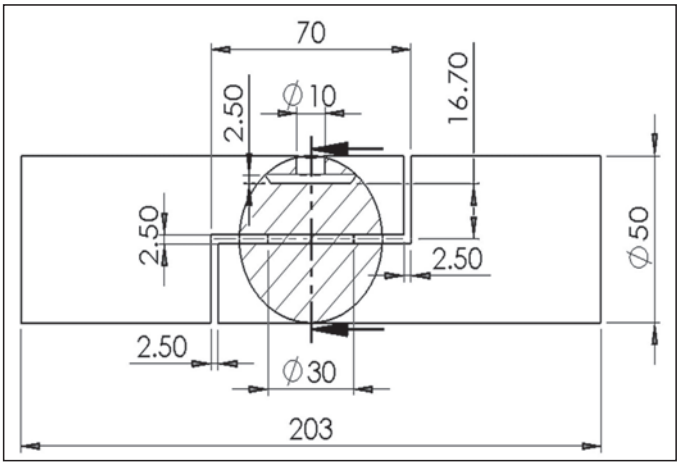

Figure 3 Cross section of simplified geometry of the globe valve (Dimensions are in mm.)

3.2 Numerical Model

Fluid flow through the globe valve is simulated, and water (properties under 25°C are taken to be analysed.) is considered as the working fluid in this thesis and assumed to be incompressible fluid. Reynold's number in this study is larger than 4000. Therefore, the flow inside the globe valve is turbulent. The governing equations are as below:

Continuity:

$$\frac{\partial \rho}{\partial t} + \frac{\partial}{\partial x_i}(\rho u_i) = 0, i = 1, 2, 3 \tag{11}$$

Momentum:

$$\frac{\partial}{\partial t}(\rho u_i) + \frac{\partial}{\partial x_j}(\rho u_i u_j) = -\frac{\partial P}{\partial x_i} + \frac{\partial}{\partial x_j}\left[\mu\left(\frac{\partial u_i}{\partial x_j} + \frac{\partial u_j}{\partial x_i}\right) - \tau_{ij}\right] \tag{12}$$

Where u represents average velocity and τ_{ij} represents Reynolds stress. Assuming the flow to be incompressible and at steady state, the equations can be expressed as:

$$\frac{\partial}{\partial x_i} u_j = 0 \tag{13}$$

$$\frac{\partial}{\partial x_i}(\rho u_j u_i - \tau_{ij}) = -\frac{\partial P}{\partial x_i} \tag{14}$$

For solving the fluid flow inside the valve, the RNG k–ε [24] model is used. Velocity inlet and outflow are set as boundary conditions for the inlet and the outlet and for wall boundary condition, standard wall function with no-slip is chosen. The SIMPLE coupling method and second-order upwind scheme under steady solutions are chosen. In this scheme, higher-order precision at the boundaries of the element is obtained by solving the Taylor center series expansion around the gravity center of the element.

4 Results and Discussion

4.1 Grid Study and Validation

As shown in Figure 4, the hybrid grid is used for meshing the geometry. In order to reduce the cost of the numerical solution while converging the results and achieve mesh independence, the geometry of the valve has meshed with 54500 nodes that is the least possible number of total nodes, which makes the results converge.

According to Polish standard PN-M-34034:1976, the value of pressure loss coefficient for a straight fully opened globe valve is 8, while other sources e.g. fitting producers or hydraulics textbooks, present lower or higher values 3 to 9.5 [1]. For a fully opened globe valve, the value of the loss coefficient presented in Fundamentals of Fluid Mechanics (B. R. Manson, 2014, page 439, Table 8.2) is reported 10. In the present work, the value of pressure loss coefficient at a fully opened state and for inlet velocity 1 m/s is obtained 8.951. It is seen that the presented calculated value of pressure loss coefficient for the globe valve is at a good accuracy and is comparable with those reported in handbooks. Also, in Ref. [1], it is expressed that the presented calculated values of pressure loss coefficients for globe valve at 33,

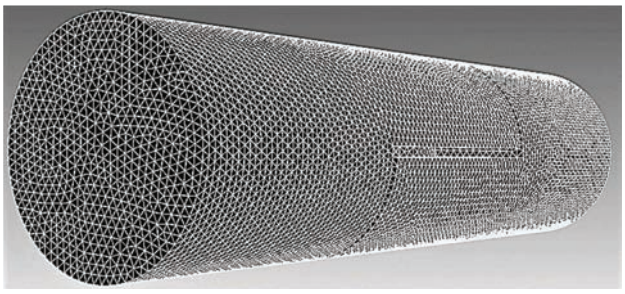

Figure 4 The computational mesh of simplified geometry of the valve.

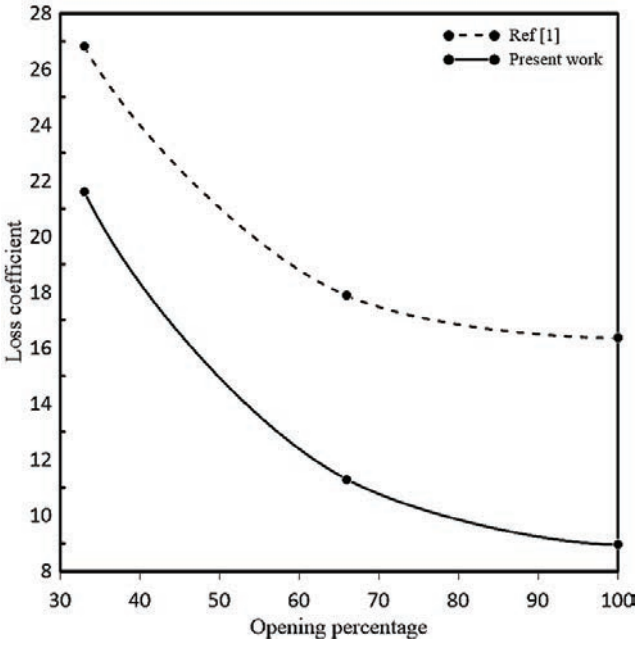

Figure 5 Validation of the numerical results.

66, and 100 opening percentage are higher than values available in common. Figure 5 shows a comparison of the results of the present work and the data of Ref. [1]. It is obvious that the current predicted results match them.

4.2 Functional Relation

In this case, the control valve is assumed fully opened. Assuming a flow rate of 1 m/s in the positive direction of the Z-axis at the input, the velocity magnitude contours is shown in Figure 6.

As shown in Figure 6, the velocity magnitude increases as the fluid pass through the valve's duct due to the reduction in cross-section area. The onset of the acceleration process is after the fluid hits the lower part of the valve's body. It is known that the flow rate and the cross-section area of the valve at the inlet and outlet are the same, so the average flow rate at the inlet and outlet of the valve will not change. However, velocity vectors in the X, Y, and Z directions will change due to changes in the geometry. The facet average velocity magnitude at the valve's outlet is obtained $V_{out} = 1.121$ m/s. As predicted, it is observed that the velocity magnitude at the outlet is increased

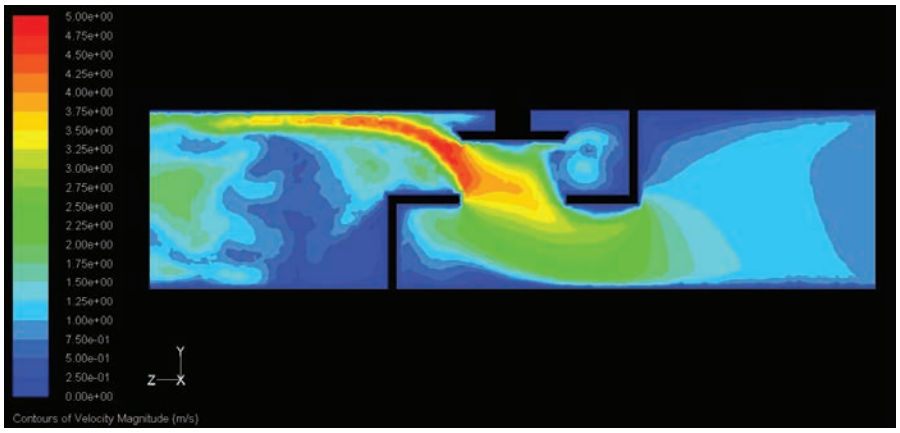

Figure 6 Velocity magnitude (m/s) contours in the middle of the valve at a fully opened state for the inlet velocity 1 m/s.

relative to the input. The Reynolds numbers at the inlet and the outlet of the valve using the Equation 1 are $\mathrm{Re}_{in} = 49810.379$ and $\mathrm{Re}_{out} = 55837.435$. As it is seen, the Reynolds number has increased at the outlet. The Reynolds number at both inlet and outlet is larger than the critical Reynolds number (2300), so the flow is turbulent. In many practical cases, the Reynolds number is larger than the critical Reynolds number and because of this, inertia effects have more influence on the flow characteristics than viscous effects. This is mostly because of the path geometry. In a path with variable areas, the fluid flow accelerates and decelerates many times and this causes that inertia effects dominate the flow characteristics. Therefore, head losses and pressure drops are associated directly with the dynamic pressure. Also, it can be concluded that in a fully developed pipe flow with a large Reynolds number, the Reynolds number doesn't affect the friction factor. The same reasoning can be expressed for flow through pipe components such as valves. Thus, the loss coefficients for valves are a function of the geometry only, $K_L = \phi(geometry)$. Therefore, in order to calculate the loss coefficient, it is necessary to analyze the pressure distribution inside the valve. The absolute pressure contours on the plate, passing through the middle of the globe valve is shown in Figure 7.

As shown in Figure 7, the flow's pressure drops after passing through the valve duct. According to the Bernoulli equation, the pressure will decrease by increasing the fluid velocity. It is clear that when the fluid passes through the valve's seat, its velocity will increase because of a reduction in the

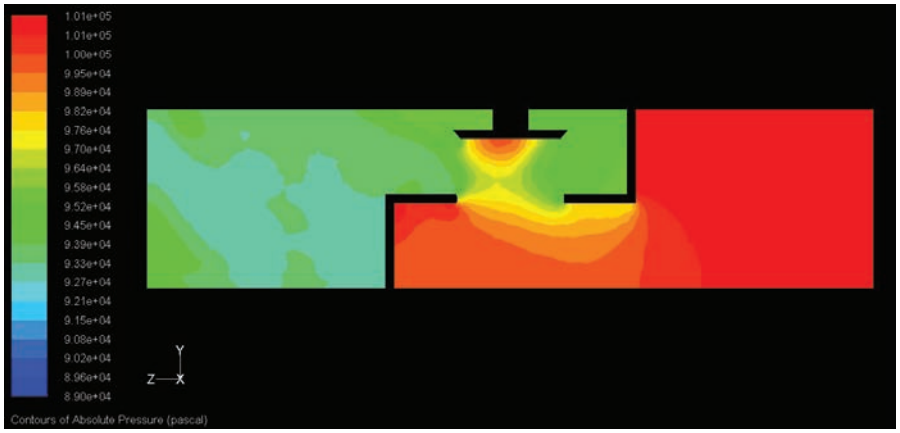

Figure 7 Absolute pressure (pascal) contours in the middle of the valve at a fully opened state for the inlet velocity 1 m/s.

passing area. This reduction in pressure can cause the pressure in the liquid to decrease to its vapor pressure. In such situations, the liquid starts to boil, and then vapor bubbles form. These bubbles move with the flow and when the pressure increases, they collapse. If this phenomenon occurs near a physical body, it can hurt the body over a period of time. The vapor pressure at 20°c is 2.338e+3 Pa, and the lowest pressure in the fully opened valve state is 8.989e+4 Pa. Therefore, cavitation will not occur inside the valve. This consideration is an important point in mechanical designs, especially in valves.

The facet average absolute pressure value at the inlet and the outlet is $P_{in} = 101326.93\ Pa$ and $P_{out} = 89891.49\ Pa$. To calculate K_L, an average velocity value of the whole valve is needed. By utilizing a numerical solution, the average velocity along the valve is obtained $V = 1.601$ m/s. By using the Equation 9, $K_L = 8.951$. Now, to derive the valve's functional relation, by changing the inlet velocity from 0 to 2.5 m/s, the values of the inlet and the outlet pressure and valve's loss coefficient at each velocity are calculated. The results are shown in Table 2.

In order to derive the valve's dimensionless functional relation, a relation that relates pressure ratio to inlet Reynolds number, it is necessary to plot the pressure ratio in terms of the inlet velocity. This relation can be very useful in choosing the best valve in a pipeline according to the valve's inlet pressure and inlet velocity. This diagram is shown in Figure 8.

Table 2 Results for different input velocities at fully opened valve state

Inlet velocity (m/s)	Inlet pressure (kpa)	Outlet pressure (kpa)	Pressure ratio	Loss coefficient
0	101.3	101.3	1	0
0.5	101.3	95.42	0.942	8.793
1	101.3	89.89	0.887	8.951
1.5	101.3	87.43	0.863	8.911
2	101.3	85.18	0.841	8.796
2.5	101.3	83.3	0.822	8.791
3	101.3	82.59	0.815	8.767
4	101.3	80.2	0.792	8.778
5	101.3	79.13	0.781	8.764

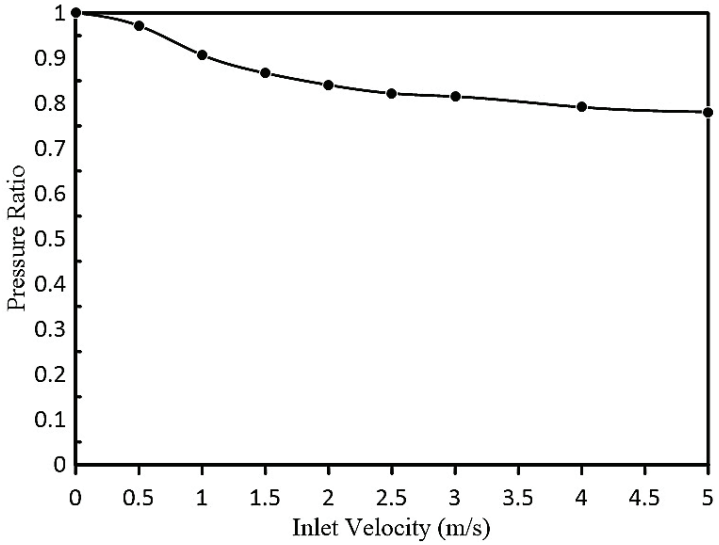

Figure 8 Pressure ratio Vs inlet velocity (m/s) at a fully opened state.

By fitting a second-order polynomial for this diagram, the dimensionless relationship between the pressure ratio and the inlet Reynolds number with a high approximation is obtained as below:

$$\frac{P_{out}}{P_{in}} = 4 \times 10^{-12}\mathrm{Re}_{in}^{2} - 2 \times 10^{-6}\mathrm{Re}_{in} + 0.9876 \tag{15}$$

Equation 15 describes the functional relation of the globe valve in the fully opened mode for water flow at different speeds. In this equation, the input pressure is known and equal to the atmosphere's pressure. Therefore,

by having the flow rate at the inlet, the outlet's average pressure can be determined.

4.3 Loss Coefficient

The velocity magnitude and absolute pressure contours at different opening states are given in Figure 9, and Table 3 shows outlet pressure, pressure ratio, and loss coefficient for the fluid flow with 1 m/s inlet velocity and at valve's different opening states.

It would be better to show the extracted results in charts. Figures 10 shows the pressure ratio and loss coefficient in terms of the globe valve's opening percentage. As it is seen in Figures 10(a) and 10(b), when the valve opens, the rate of change in pressure ratio and loss coefficient are very sharp and change quickly. Gradually, this rate decreases and the results tend to the final value at valves fully opened state. This is quite true because when the valve opens, the valve's plug has a significant effect on the fluid's flow. And finally, when the valve is fully opened, the valve's plug is placed at the highest point of the valve, and as a result, its effect on the flow is less than before. Therefore, the impact of the valve's geometry on the flow is an important part of analyzing the flow's behavior inside it and should be taken into account.

One way to determine whether the results in a particular case are correct or not is to extract the results in several cases and compare them with that particular case. Results for inlet velocity 2, 3, 4, and 5 m/s at different opening states are listed in Table 4.

Pressure ratio Vs opening percentage for different inlet velocities is shown in Figure 11. As it is seen in Figure 11, the general trend of the chart at all inlet velocities is the same. In this way, at first, the process of changing the

Table 3 Results for inlet velocity 1 m/s at different opening states

Opening percentage	Inlet pressure (kpa)	Outlet pressure (kpa)	Pressure ratio	Loss coefficient
0	101.3	0	0	∞
5	101.3	3.829	0.038	682.3
10	101.3	9.895	0.098	163.4
15	101.3	21.12	0.208	73.41
20	101.3	41.42	0.409	39.1
25	101.3	67.09	0.662	25.5
50	101.3	84.91	0.839	13.35
75	101.3	88.84	0.877	10.14
100	101.3	89.89	0.887	8.951

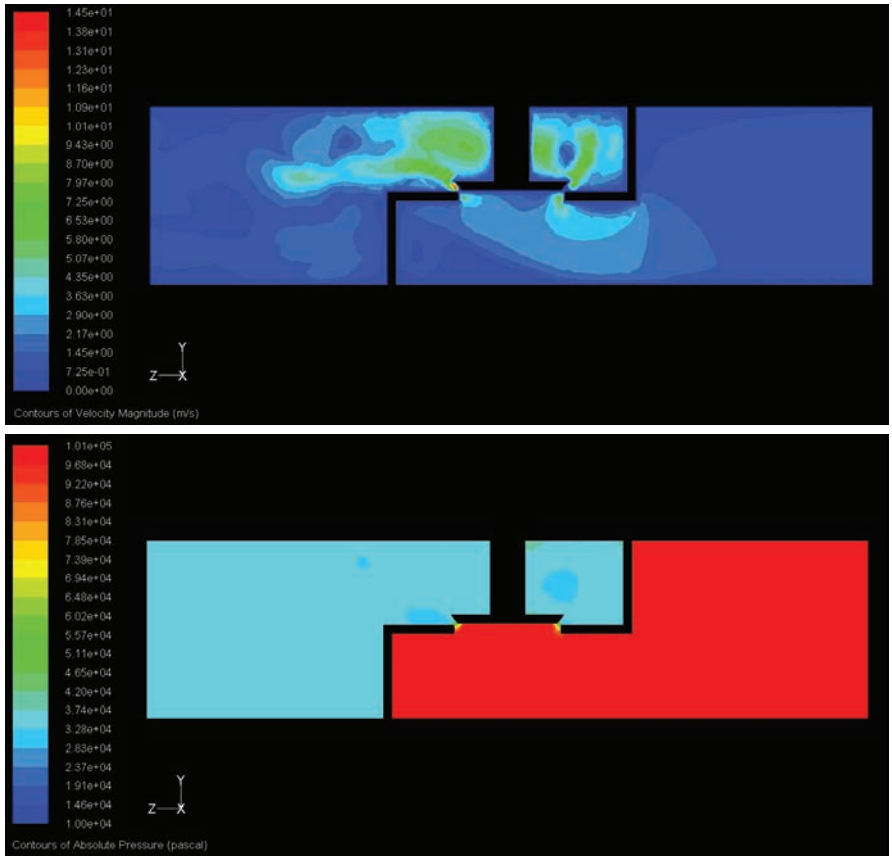

a) 10% Open

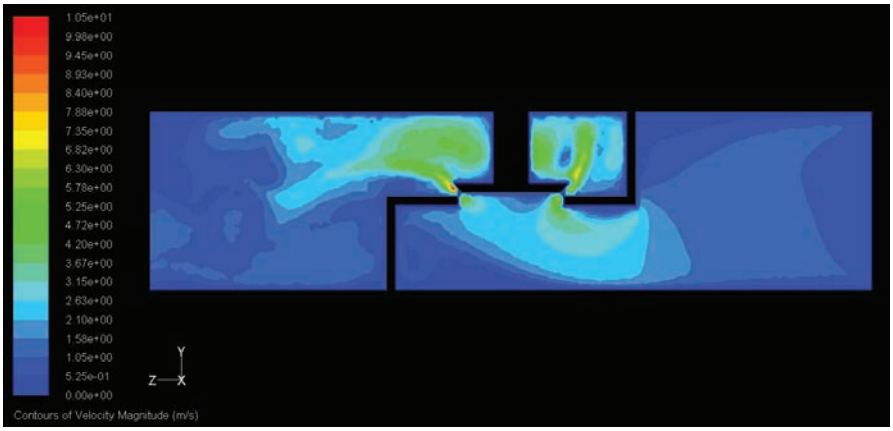

Figure 9 (Continued)

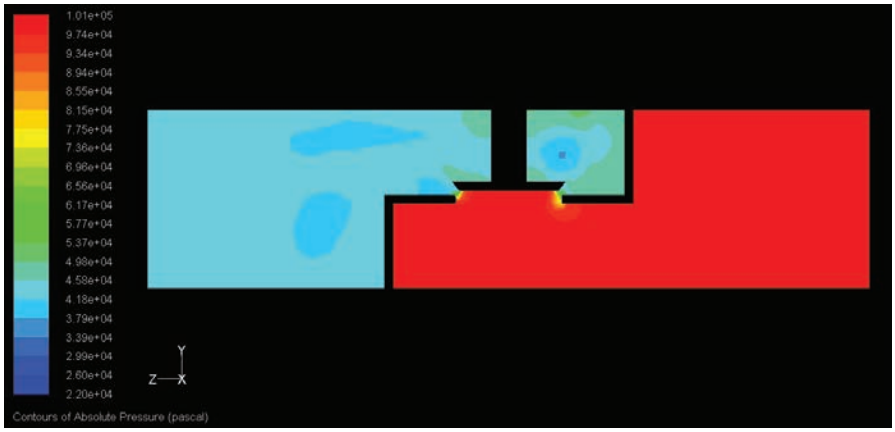

b) 15% Open

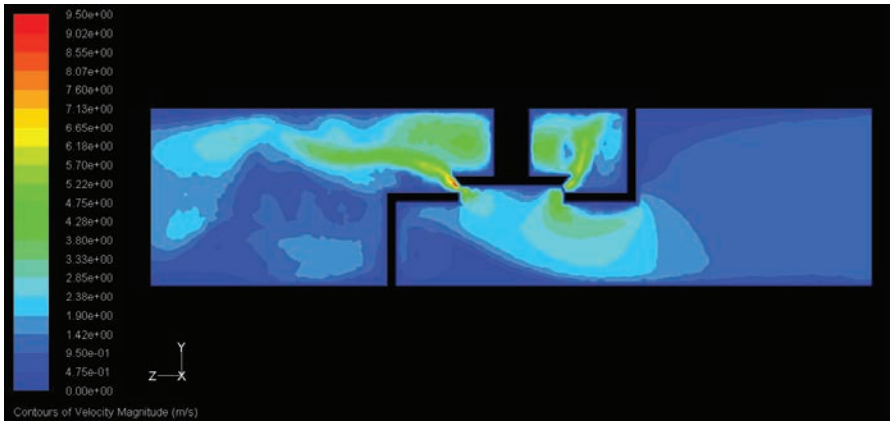

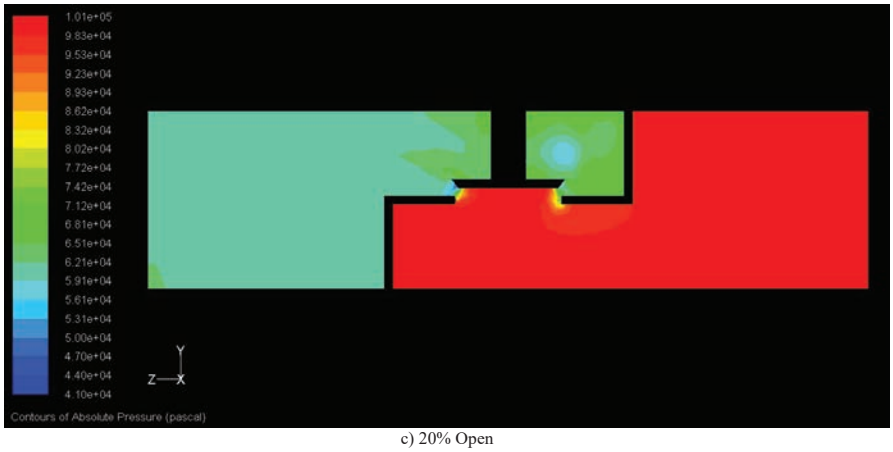

c) 20% Open

Figure 9 (Continued)

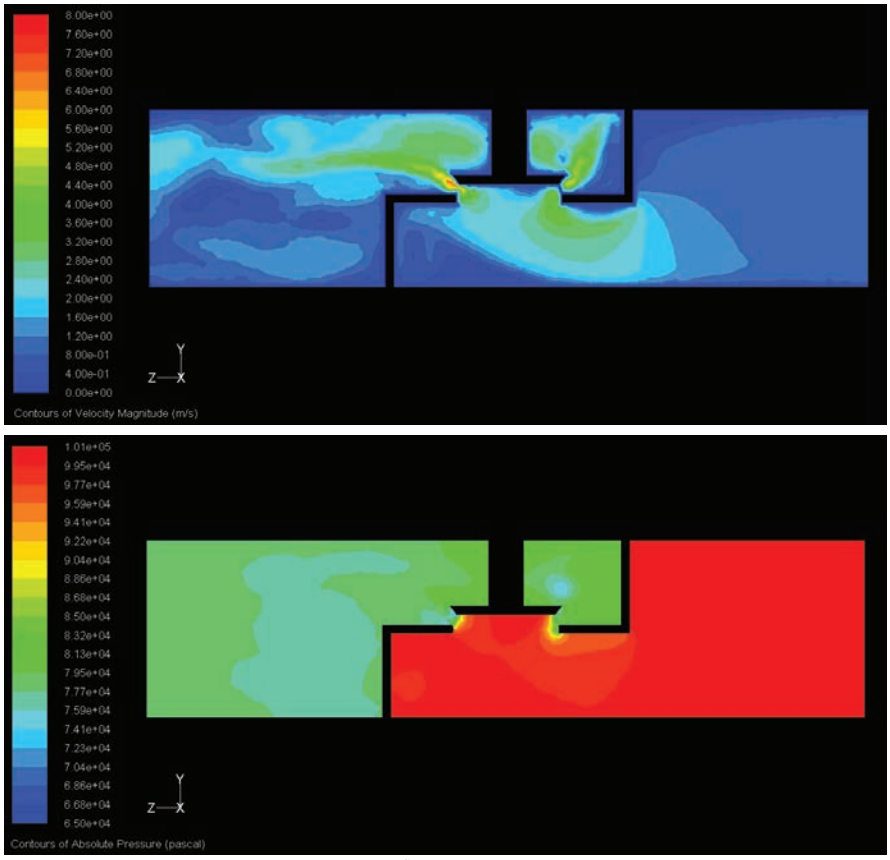

d) 25% Open

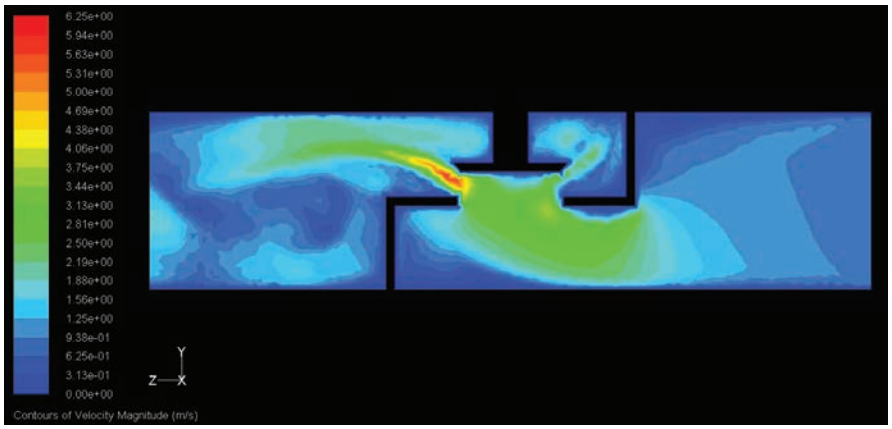

Figure 9 (Continued)

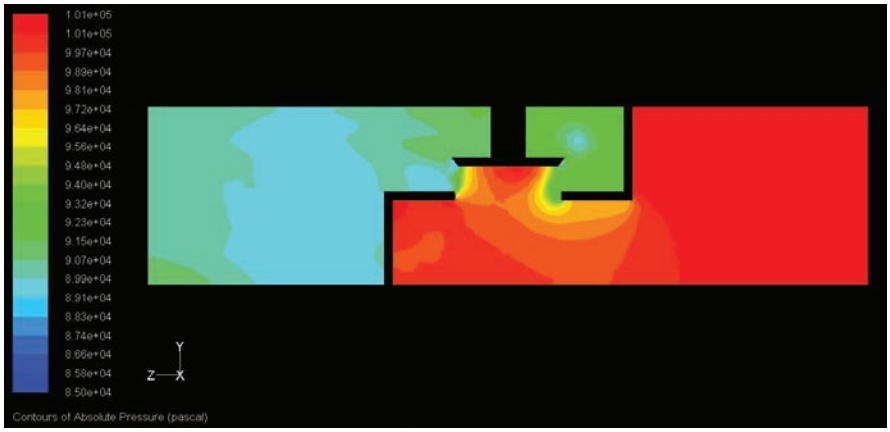

e) 50% Open

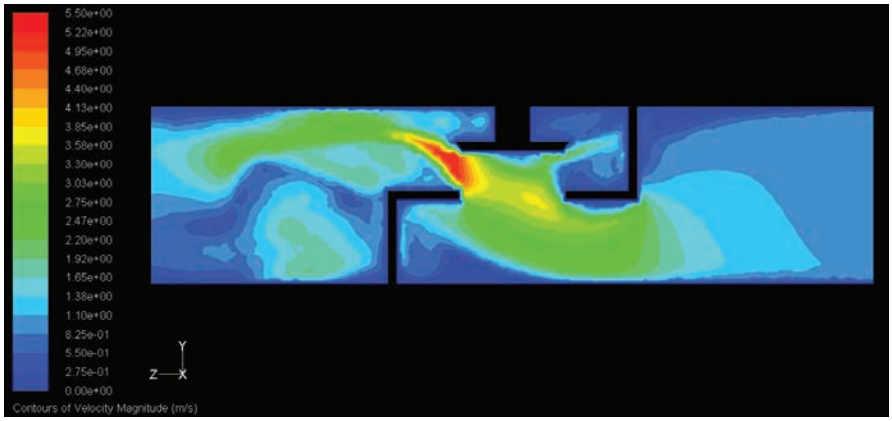

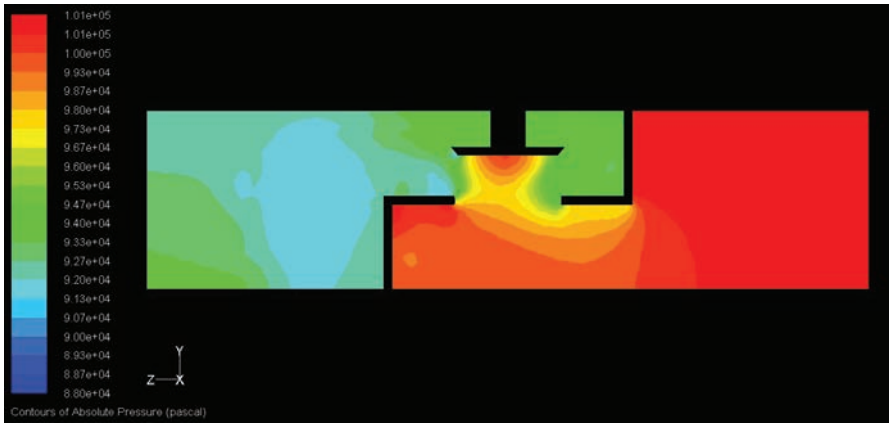

f) 75% Open

Figure 9 (Continued)

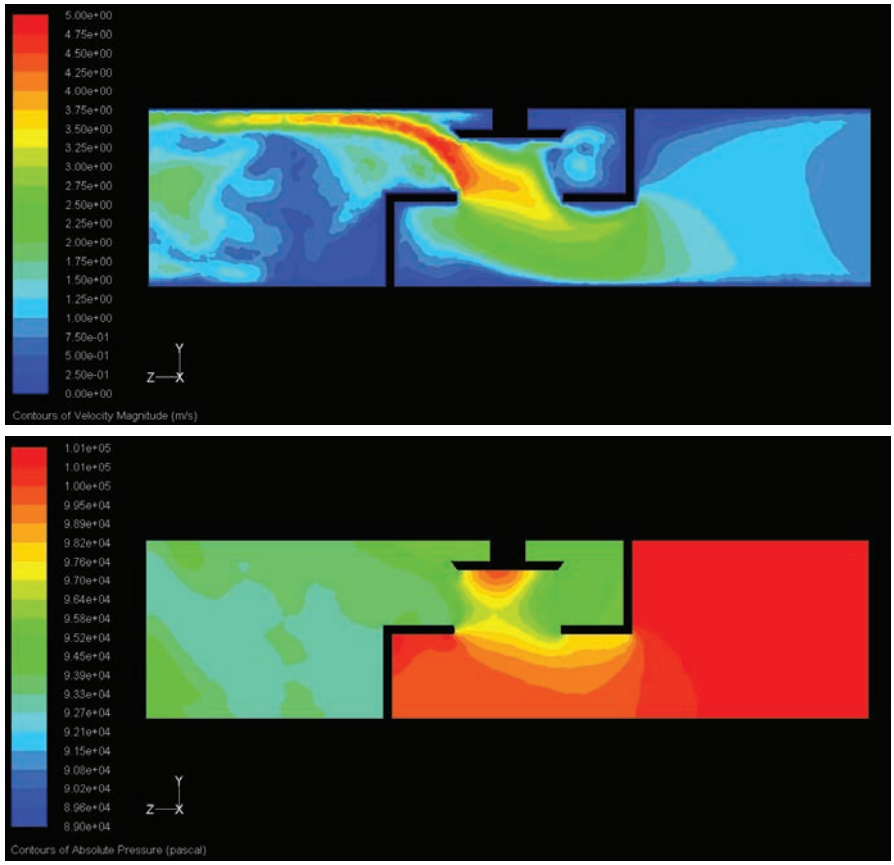

g) 100% Open

Figure 9 Velocity (left) and pressure (right) contours at different opening states for inlet velocity 1 m/s.

pressure ratio is very sharp, and gradually the pressure ratio tends to the final value at the valve fully opening state. In addition, in each opening percentage, the pressure ratio decreases as the inlet velocity increases.

Figure 12 shows loss coefficient Vs opening percentage for inlet velocity 1, 2, 3, 4, and 5 m/s. It is clear that for different inlet velocities, the loss coefficient decreases sharply when the valve opens and then tends to the final value. Also, at each opening percentage, the value of the loss coefficient for different inlet velocities are almost equal to each other.

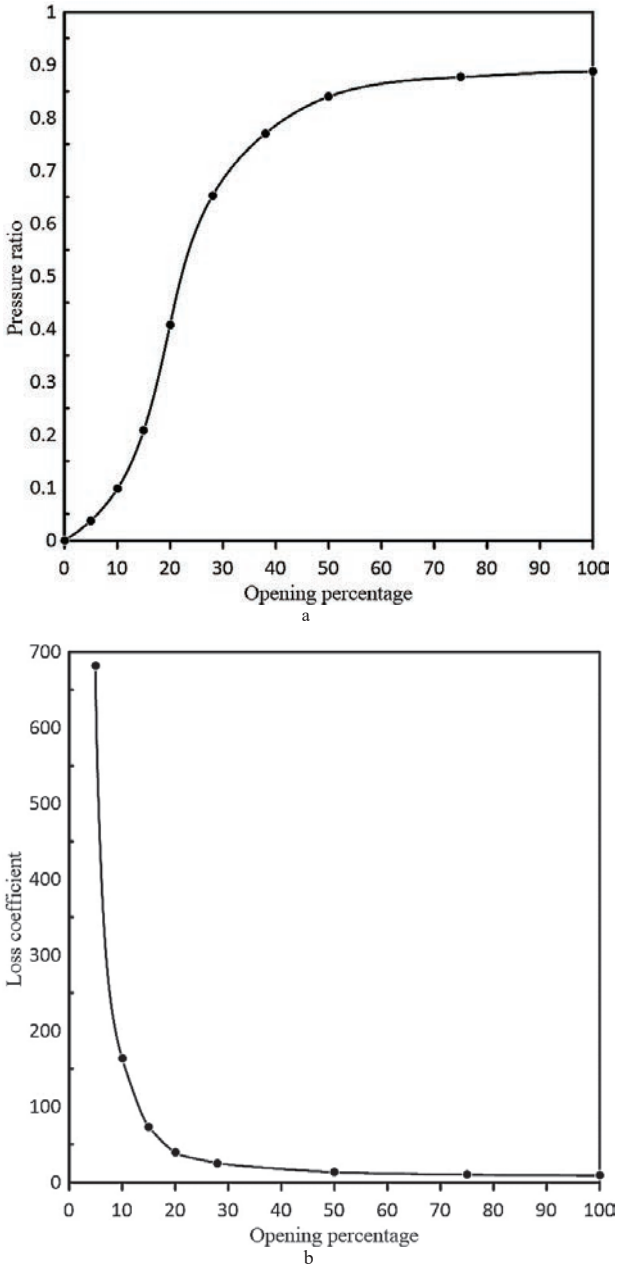

Figure 10 (a) Pressure ratio and (b) loss coefficient Vs opening percentage for inlet velocity 1 m/s.

Table 4 Results for inlet velocity 2, 3, 4, and 5 m/s at different opening states

Opening percentage			0	5	10	15	20	25	50	75	100
Velocity (m/s)	2	Outlet press. (kpa)	0	2.969	8.927	18.61	36.63	62.8	81.1	85.09	85.18
		Press. ratio	0	0.029	0.088	0.184	0.362	0.619	0.8	0.839	0.841
		Loss Coef.	∞	682.9	163.7	73.42	39.22	25.61	13.21	10.13	8.796
	3	Outlet press. (kpa)	0	2.148	8.542	17.47	33.75	59.81	78.14	81.36	82.59
		Press. ratio	0	0.021	0.084	0.172	0.333	0.59	0.771	0.803	0.815
		Loss Coef.	∞	682.6	163.5	73.9	39.14	25.79	13.39	10.14	8.77
	4	Outlet press. (kpa)	0	1.55	8.218	16.59	31.6	57.64	76.21	79.05	80.2
		Press. ratio	0	0.015	0.081	0.164	0.312	0.569	0.752	0.78	0.791
		Loss Coef.	∞	683	164.1	73.71	39.18	25.58	13.4	10.29	8.778
	5	Outlet press. (kpa)	0	1.327	7.944	15.68	30.45	55.84	75.15	77.97	79.13
		Press. ratio	0	0.013	0.075	0.155	0.3	0.551	0.742	0.769	0.781
		Loss Coef.	∞	682.9	164.3	74	39.2	25.7	13.39	10.3	8.764

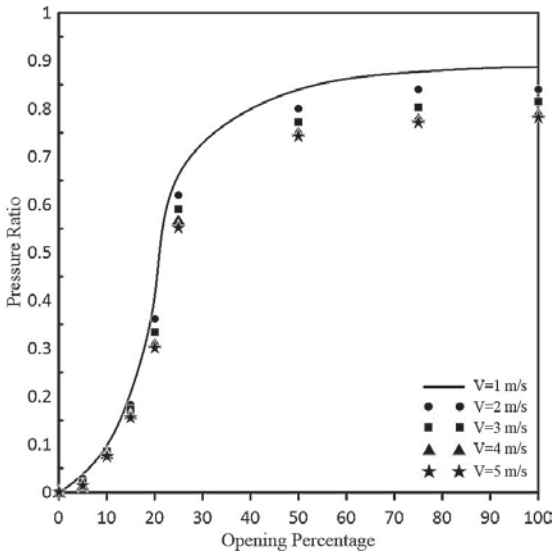

Figure 11 Pressure ratio Vs opening percentage for inlet velocity 1, 2, 3, 4, and 5 m/s.

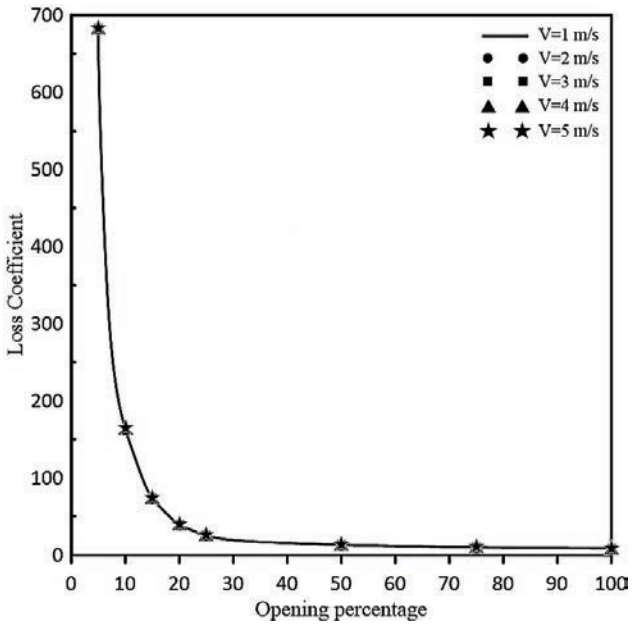

Figure 12 Loss coefficient Vs opening percentage for inlet velocity 1, 2, 3, 4 and 5 m/s.

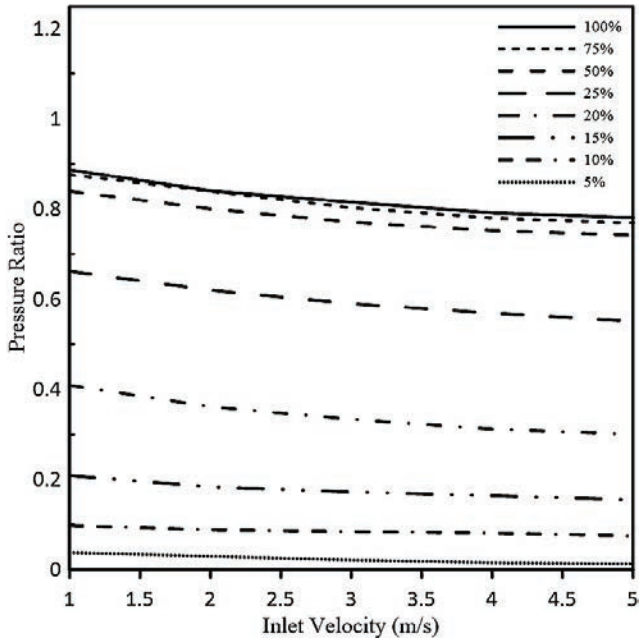

Figure 13 Pressure ratio Vs inlet velocity (m/s) at different opening valve states.

Pressure ratio Vs inlet velocity at different opening valve states is indicated in Figure 13. According to Figure 13, it can be seen that the pressure ratio at each opening percentage decreases by increasing the inlet velocity. This reduction is also obvious in Figure 11. By increasing the inlet velocity, the rate of this reduction decreases. This means that the pressure ratio at high inlet velocities is independent of the inlet velocity changes. In addition, by changing the valve's position from a fully closed to a fully opened state, the value of pressure ratio increases from 0.05 to almost 0.9 at each inlet velocities.

5 Conclusion

In the present paper, a 3-D globe valve is modeled and then simulated to extract its functional relation and estimate its loss coefficient by numerical solution in order to obtain the functions of the flow through the valve according to pressure and the valve's opening state by using the results and also estimate its loss coefficient at different valve's opening states which were not

covered comprehensively in previous articles. It is clearly observed that the valve's geometry has a direct impact on the fluid characteristics which passes through it. The important parts of a valve which have the most influence on the fluid flow are the plug and the seat. According to the obtained results,

1. The globe valve's loss coefficient at different opening states is estimated which can be very useful for the selection and usage of globe valves under certain conditions.
2. Pressure ratio and loss coefficient are functions of the valve's opening percentage and inlet velocity. When the valve opens, the rate of change in outlet velocity, pressure, and loss coefficient is very sharp. The value of outlet velocity and pressure increases at a sharp rate, and the loss coefficient decreases sharply. After the valve is approximately 20% open, the rate of these changes decreases, and the results approximately tend to the final value at a fully opened state.
3. Another important point is that the outlet pressure is a function of inlet velocity and decreases when the inlet velocity increases. This makes it possible to estimate the outlet pressure at a very good approximation by having the fluid flow rate at the inlet of the valve.

Also, further studies can be done in this field. In the present work, a simplified model of a globe valve was investigated. By improving the geometric model of the globe valve, better numerical results can be achieved.

References

[1] C. Co, *Flow of Fluids*. Technical paper 410, 1988.

[2] J. A. Davis and M. Stewart, "Predicting globe control valve performance – Part 1: CFD modeling," *J Fluids Eng-Trans ASME*, vol. 124, no. 3, pp. 772–777, 2002.

[3] J. A. Davis and M. Stewart, "Predicting Globe Control Valve Performance – Part II: Experimental Verification," *Journal of Fluids Engineering*, vol. 124, no. 3, pp. 778–783, 2002.

[4] Z. Lin, H. Wang, Z. Shang, B. Cui, C. Zhu, and Z. Zhu, "Effect of cone angle on the hydraulic characteristics of globe control valve," *Chin. J. Mech. Eng.*, vol. 28, no. 3, pp. 641–648, 2015.

[5] C. Long and J. Guan, "A method for determining valve coefficient and resistance coefficient for predicting gas flowrate," *Exp. Therm. Fluid Sci.*, vol. 35, no. 6, pp. 1162–1168, 2011.

[6] M.-J. Chern and C.-C. Wang, "Control of Volumetric Flow-Rate of Ball Valve Using V-Port," *Journal of Fluids Engineering*, vol. 126, no. 3, pp. 471–481, 2004.
[7] A. D. Toro, M. C. Johnson, and R. E. Spall, "Computational Fluid Dynamics Investigation of Butterfly Valve Performance Factors," *J. – Am. Water Works Assoc.*, vol. 107, no. 5, pp. 243–254, 2015.
[8] F. Haque, F. Haider, A. Rahman, and Q. Islam, "Study of different types of valves & Determination of Minor Head Loss for various openings of locally available plastic valve," in *Proceedings of the 13th Asian Congress of Fluid Mechanics*, 2010, pp. 605–608.
[9] A. Tabrizi, M. Asadi, G. Xie, G. Lorenzini, and C. Biserni, "Computational fluid-dynamics-based analysis of a ball valve performance in the presence of cavitation," *Journal of Engineering Thermophysics*, vol. 23, no. 1, pp. 27–38, 2014.
[10] S. F. Moujaes and R. Jagan, "3D CFD predictions and experimental comparisons of pressure drop in a ball valve at different partial openings in turbulent flow," *Journal of Energy Engineering*, vol. 134, no. 1, pp. 24–28, 2008.
[11] B. Cui, Z. Lin, Z. Zhu, H. Wang, and G. Ma, "Influence of opening and closing process of ball valve on external performance and internal flow characteristics," *Experimental Thermal and Fluid Science*, vol. 80, pp. 193–202, 2017.
[12] V. Fester, D. Kazadi, B. Mbiya, and P. Slatter, "Loss coefficients for flow of Newtonian and non-Newtonian fluids through diaphragm valves," *Chemical Engineering Research and Design*, vol. 85, no. 9, pp. 1314–1324, 2007.
[13] T. Kimura, T. Tanaka, K. Fujimoto, and K. Ogawa, "Hydrodynamic characteristics of a butterfly valve – prediction of pressure loss characteristics," *ISA transactions*, vol. 34, no. 4, pp. 319–326, 1995.
[14] J.-y. Qian, L. Wei, Z.-j. Jin, J.-k. Wang, and H. Zhang, "CFD analysis on the dynamic flow characteristics of the pilot-control globe valve," *Energy conversion and management*, vol. 87, pp. 220–226, 2014.
[15] Z.-j. Jin, Z.-x. Gao, M. Zhang, and J.-y. Qian, "Pressure drop analysis of pilot-control globe valve with different structural parameters," *Journal of Fluids Engineering*, vol. 139, no. 9, 2017.
[16] J. H. Lee, X. G. Song, S. M. Kang, and Y. C. Park, "Optimization of Flow Coefficient for Pan Check Valve by Fluid Dynamic Analysis," in *AIP Conference Proceedings*, 2010, vol. 1239, no. 1, pp. 337–340: American Institute of Physics.

[17] X. Song, L. Wang, and Y. Park, "Fluid and structural analysis of large butterfly valve," in *AIP Conference Proceedings*, 2008, vol. 1052, no. 1, pp. 311–314: American Institute of Physics.

[18] X. Lv, B. K. Saha, Y. Wu, and S. Li, "Distributed parameters modeling for the dynamic stiffness of a spring tube in servo valves," *Structural Engineering and Mechanics*, vol. 75, no. 3, pp. 327–337, 2020.

[19] W. Huang, J. Ren, and A. Forooghi, "Vibrational frequencies of FG-GPLRC viscoelastic rectangular plate subjected to different temperature loadings based on higher-order shear deformation theory and utilizing GDQ procedure," *Mechanics Based Design of Structures and Machines*, pp. 1–26, 2021.

[20] Y. Bai, M. Suhatril, Y. Cao, A. Forooghi, and H. Assilzadeh, "Hygro–thermo–magnetically induced vibration of nanobeams with simultaneous axial and spinning motions based on nonlocal strain gradient theory," *Engineering with Computers*, pp. 1–18, 2021.

[21] Y. Kerboua, A. Lakis, M. Thomas, and L. Marcouiller, "Computational modeling of coupled fluid-structure systems with applications," *Structural Engineering and Mechanics*, vol. 29, no. 1, pp. 91–112, 2008.

[22] V. Ghazanfari, A. A. Salehi, A. R. Keshtkar, M. M. Shadman, and M. H. Askari, "Numerical Simulation Using a Modified Solver within OpenFOAM for Compressible Viscous Flows," *European Journal of Computational Mechanics*, pp. 541–572–541–572, 2019.

[23] B. Munson, D. Young, and T. Okiishi, *Fundamentals of Fluid Mechanics*. 1998.

[24] V. Yakhot and S. A. Orszag, "Renormalization group analysis of turbulence. I. Basic theory," *Journal of scientific computing*, vol. 1, no. 1, pp. 3–51, 1986.

Biography

Saber Rezaey is a master of science student in aerospace engineering at Tarbiat Modares University, Tehran, Iran. He received his bachelor of science in mechanical engineering from Zanjan University, Zanjan, Iran. His research interests include fluid mechanics, computational fluid dynamics (CFD), fluid-structure interaction, aerodynamic, and wind turbine aerodynamics.